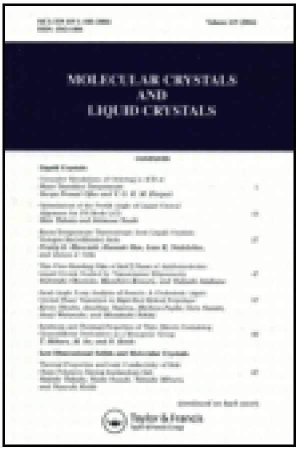

Molecular Crystals and Liquid Crystals Science and Technology. Section A. Molecular Crystals and Liquid Crystals

Publication details, including instructions for authors and subscription information:
http://www.tandfonline.com/loi/gmcl19

Analysis of the Operation of Mixed-Mode Twisted Nematic Cells

Kun-Wei Lin [a] , Jinn-Chou Yoo [a] & Han-Ping D. Shieh [a]

[a] Institute of Electro-optical Engineering, National Chiao Tung University , Hsin-Chu, Taiwan, Rep. of China

Published online: 04 Oct 2006.

Mol. Cryst. Liq. Cryst., 1997, Vol. 293, pp. 29–38
Reprints available directly from the publisher
Photocopying permitted by license only

Analysis of the Operation of Mixed-Mode Twisted Nematic Cells

KUN-WEI LIN, JINN-CHOU YOO and HAN-PING D. SHIEH

Institute of Electro-optical Engineering, National Chiao Tung University, Hsin-Chu, Taiwan, Rep. of China

(Received 25 April 1996; In final form 9 August 1996)

Analysis of mixed-mode twisted nematic (MTN) cells in one- and two-dimension simulation are presented. Two-dimensional simulation reveals that the light leakage in the region of the reverse tilt domain in MTN cells reduces the contrast ratio with a novel method by adding a bias voltage onto Silicon substrates, the light leakage can be suppressed and the open ratio of the cell is greatly improved.

Keywords: Reflective liquid crystal displays; mixed-mode twisted nematic cells; unhomogeneous electrical field; open ratio

INTRODUCTION

Liquid crystal display projectors (LCPJs) have found extensive applications in large screen displays. Compactness, light weight, and high image quality are among the major advantages. However, how to further improve the optical efficiency and enhance the resolution are still among important issues. Among the variety of LCD projectors, the reflective-type operation has advantages of high open ratio (>85%) and efficient utilization of the unpolarized light by a polarization beam splitter [1,2]. Recently, a new mixed-mode twist nematic liquid crystal (MTN) cell has been proposed for reflective-type LCPJs of high optical efficiency [3]. The MTN cell is shown to be relatively promising in optical performance for one-dimensional reflective-mode operation. The reflectance versus voltage curve (R-V curve) is relatively insensitive to the wavelength of incident light and a dark state can be achieved for R, G, and B pixels at high operation voltage. However, LC director deformation under an unhomogenous electric field produced by multi-electrodes can result in reverse tilt domains occurring in the pixel area to reduce the open ratio of a pixel, thus to degrade the optical performance.

Typical configurations of MTN cells have been analyzed in this study by calculating two-dimensional LC molecule orientations under different driving methods to compare their optical performance. An LC continuum theory implemented by a tensor taking elastic anisotropy and unhomogeneous electric field into consideration is used to calculate the two-dimensional LC molecule orientations in MTN cells [4, 5]. Besides, the reflectance of MTN cells are calculated by the extended Jones Matrix [6]. Therefore, the optimized operation of MTN cells to have a higher reflectance and less color deviation can be achieved. Moreover, a novel driving method has been proposed to suppress the light leakage caused by the reverse tilt domain and, as a result, the open ratio is greatly improved.

MTN-90° CELLS

The configurations of MTN-90° cells are similar to conventional 90° TN cells, except that MTN-90° cells have lower retardation ($d\Delta n$) and their front LC directors are set at an angle β with respect to the polarization state of incident light. Since $d\Delta n$ of MTN-90° cells is less than that of normal 90° TN cells, the polarization state of incident light will not follow the adiabatic process to fully rotate 90 degrees as does that of conventional 90° TN cells. Angle β further enhances the birefringence effect of the MTN-90° cells. Therefore, there are two operation modes occurring in MTN-90° cells: polarization rotation and birefringence effect. By properly mixing the two effects, the functionality of MTN-90° cells can be treated as an achromatic quarter-wave plate.

In order to illustrate the basic characteristic of the MTN-90° cells, the maximum reflectance as a function of $d\Delta n$ of LC has been calculated with respect to a given angel β. The LC parameters used in this calculation are listed in Table I. We varied angle β until it reached the maximum reflectance at a given $d\Delta n$ of MTN-90° cells. The maximum reflectance as a function of $d\Delta n$ of MTN-90° cells at three incident wavelengths of R (620 nm), G (540 nm), and B (460 nm) is depicted in Figure 1(a). Although the global maximum reflectance occurs at $\beta = 56°$ where $d\Delta n$ is much larger than that of the local maximum of $\beta = 20°$, the color deviation becomes more severe. By selecting $d\Delta n = 0.25$ μm and $\beta = 20°$, reflectance as a function of applied voltage at R, G, and B pixel is shown in Figure 1(b). The

TABLE I Parameters of MTN cells used for calculations

LC parameters:
$K_{11} = 16.1\text{pN}$, $K_{22} = 7.0\text{pN}$, $K_{33} = 21.4\text{pN}$
$\varepsilon\perp = 4.0$, $\varepsilon = 14.1$, $n_e = 1.739$, $n_o = 1.52$
Boundary conditions:
pretilt angle = 3°, twist angle = 90°
β(front panel (ITO) to the y axis) = 20°

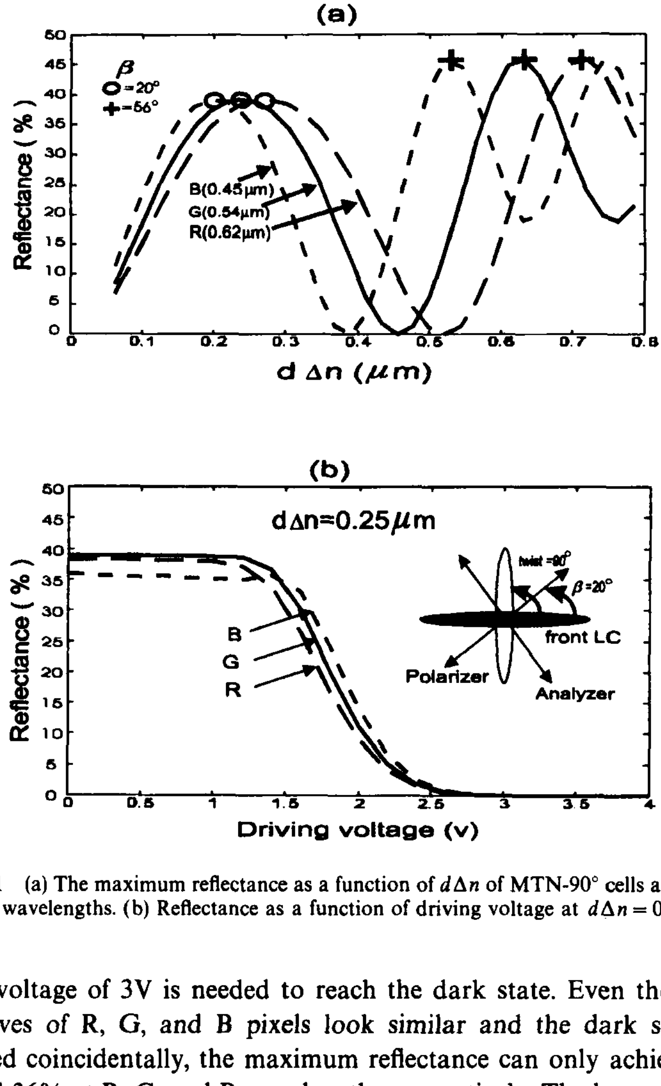

FIGURE 1 (a) The maximum reflectance as a function of $d\Delta n$ of MTN-90° cells at R, G, and B incident wavelengths. (b) Reflectance as a function of driving voltage at $d\Delta n = 0.25\,\mu\text{m}$ and $\beta = 20°$.

applied voltage of 3V is needed to reach the dark state. Even though the R-V curves of R, G, and B pixels look similar and the dark states are converged coincidentally, the maximum reflectance can only achieve 38%, 39% and 36% at R, G, and B wavelengths, respectively. The low reflectance can be overcome by low-twisted nematic (LTN) cells to be described in following section.

MTN-80° AND MTN-70° CELLS

Low-twisted (LTN) cells have been shown to possess lower $d\Delta n$ than conventional 90° TN-cells when both are at maximum transmittance [7]. Moreover, the LTN cells need a higher driving voltage than normal 90° TN-cells to reach the dark state. The characteristics of LTN cells can be implemented with the MTN mode. The results are shown in Figures 2(a) and 2(b) for the case of MTN-80° cells. In order to reach the first local maximum of MTN-80° cells, $d\Delta n$ and β are 0.23 µm and 18°, respectively.

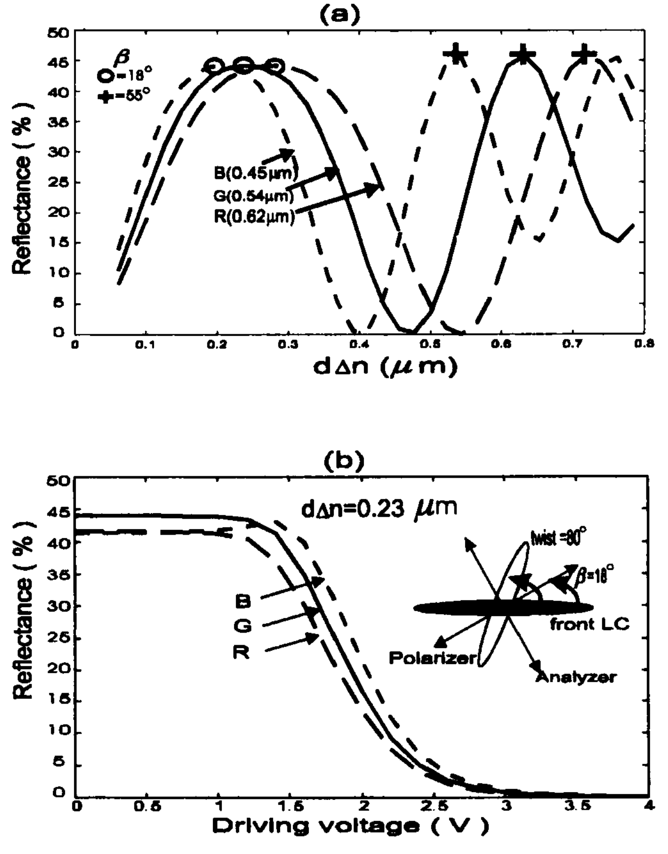

FIGURE 2 (a) The maximum reflectance as a function of $d\Delta n$ of MTN-80° cells. (b) Reflectance as a function of driving voltage at $d\Delta n = 0.23$ µm and $\beta = 18°$.

Compared with MTN-90° cells, the reflectance at the first local maximum at R, G, and B wavelengths has been improved up to 44%, 42%, and 42%, respectively. For the case of MTN-70° cells, the first local maximum reflectance occurs at $d\Delta n$ of 0.22 μm and β of 16°, shown in Figure 3(a), and the maximum reflectance of MTN-70° cells has been further improved to 46%, 44%, and 44% at R, G, and B wavelengths, as revealed in Figure 3(b). However, applied voltages of 4 and 5V are needed to reach the dark states for MTN-80° and -70° cells, respectively.

OPTICAL PERFORMANCE OF 2D-DEFORMED MTN-90° CELLS

It is known that the unhomogenity of the electrostatic field in the LCDs causes the distribution of the director orientation to be discontinuous, thus

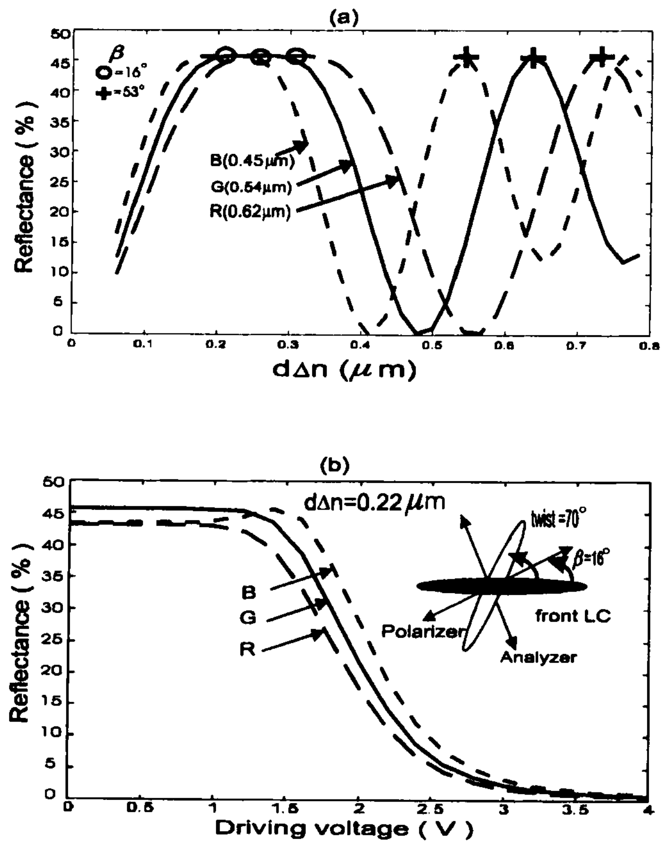

FIGURE 3 (a) The maximum reflectance as a function of $d\Delta n$ of MTN-70° cells. (b) Reflectance as a function of driving voltage at $d\Delta n = 0.22$ μm and $\beta = 16°$.

it degrades the performance of the display. A two-dimension simulation is used to calculate the distribution of the nematic director orientation and the reflectance of MTN-90° cells is illustrated in Figure 4. The front LC director is set at an angle β of 20° to the polarization state (y-axis) of the incident light. The driving circuits are fabricated on Silicon substrates and isolated by Si_3N_4 from the LC molecules. Each pixel is defined by aluminum coating on the Si_3N_4. The simulation area is divided into three pixels with the same structure.

The fringe effect significantly affects the optical performance of the cell at high applied voltage. Since the lateral component of the electric field in the region near the edge of the pixel electrode is quite different with respect to driving methods, three kinds of driving methods, dot inversion, frame inversion, and frame inversion with a bias voltage on the silicon substrate have been investigated to compare their optical properties. Two voltage pairs of (−3, 2.8, −3V) and (3, 2.8, 3V) are applied to the three pixels driven by dot and frame inversion methods. The resultant nematic directors and equal potential contours driven by the dot inversion method are shown in Figures 5(a) and 5(b), respectively. The electric field tends to align the LC directors (denoted by arrows) perpendicular with respect to the potential contour lines. The directions of the fringe electric field produced at the left and right edges of the pixel electrode are opposite to each other. The LC directors therefore tilt in opposite directions near the two edges of the pixel electrode. The LC molecules are divided into two regions under the pixel electrode and the reverse tilt region occurs on the left side, as shown in Figure 5(a).

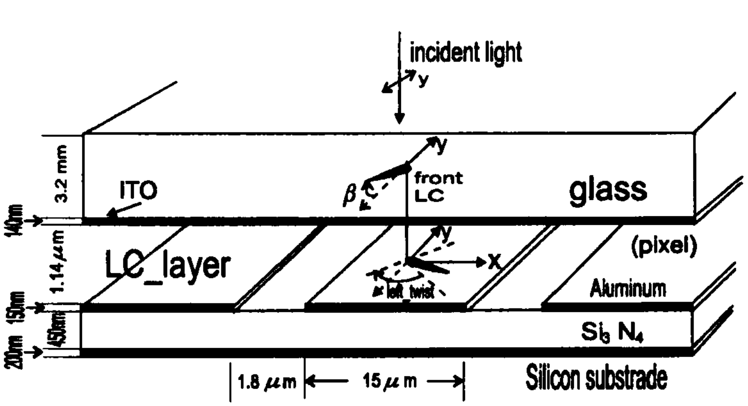

FIGURE 4 The 2-D MTN-90° cells used to calculate the distribution of the nematic director orientation and the reflectance. The front LC director is set at an angle β of 20° to the polarization state (y-axis) of the incident light.

The reflectance profile for the case of Figure 5(a) is shown in Figure 5(c). Reflectance of most of the area of the two side pixels and the middle pixel is about 0.3%, and 1%, respectively. However, there are abnormal reflectance around the edges between two pixels, especially, a reflectance as high as 26% occurs in the region of the reverse tilt domain. The abnormal reflectance caused by the fringe field reduces contrast and should be masked by a black matrix. The open ratio, defined as the ratio between the normal reflectance area to the pixel pitch, is around 70%, as shown in Figure 5(c).

Similarly, the resultant nematic directors and equal potential contours driven by the frame inversion method are shown in Figures 6(a) and 6(b), respectively. The reverse tilt domain is moved slightly to the left edge of the pixel electrode, as shown in Figure 6(a). Reflectance profiles are quite different from those of the dot inversion method in the region between pixels, as shown in Figure 6(c). This is due to the fact that the strong lateral electric field produced by the dot inversion method tends to force the LC molecules to align vertically with the edge of pixel electrode, hence, to reduce the phase retardation of the MTN cell to null. In contrast, the lateral electric

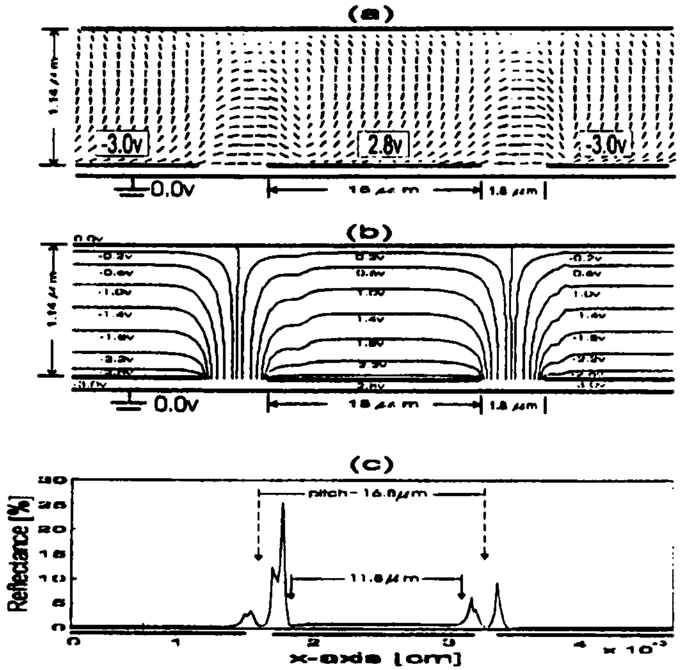

FIGURE 5 (a) The calculated LC directors projected onto x-y plane driven by the dot inversion method. (b) Calculated equal potential contours. (c) 2-D reflectance profile reveals that abnormal reflectance occurred in the region of pixel edges.

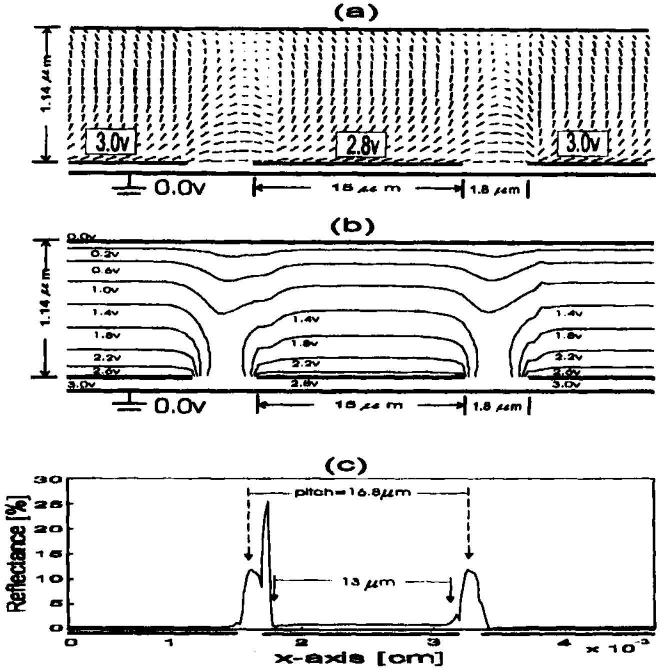

FIGURE 6 (a) The LC directors driven by the frame inversion method. (b) Calculated equal potential contours. (c) 2-D reflectance profile exhibits that the fringe field effect is quite different between the dot and frame inversion methods.

field has less effect on LC molecules driven by the frame inversion method. As a result, the open ratio improved to 77%.

To further suppress the abnormal reflectance profiles, both the dot and frame inversion methods with a bias voltage on the substrate have been investigated. In our simulation, the bias voltage has less effect on the LC directors and their optical performance by the dot inversion method. In constrast, the bias voltage significantly affects the LC directors in the region between pixels driven by the frame inversion method. When the bias voltage of 3V is applied, the resultant nematic directors and equal potential contours, shown in Figures 7(a), and 7(b), reveal that the reverse tilt domain has vanished and the LC directors are rather uniform throughout entire LC layer. The reflectance profile, depicted in Figure 7(c), shows that light leakage in the pixel electrode area has almost been eliminated. As a result, the open ratio is greatly improved to 89%.

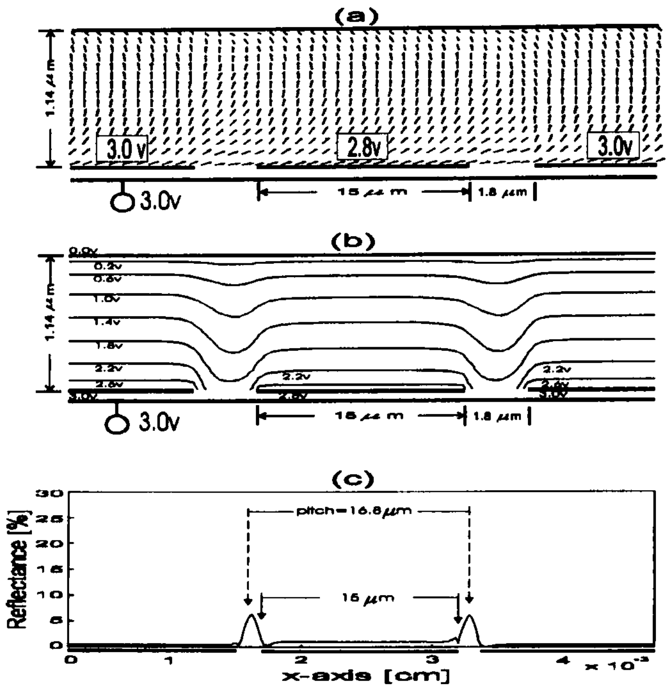

FIGURE 7 (a) The LC directors for the frame inversion method with a bias voltage of 3V on the substrate. (b) Calculated equal potential contours. (c) 2-D reflectance profile shows that the light leakage has been suppressed in the region of the pixel electrode.

CONCLUSION

By proper mixing of two operations, polarization rotation and birefringence effects, a MTN cell can be implemented as an achromatic quarter-wave plate to the reflective-type projection display. We have analyzed the working principle of mixed-mode twisted nematic (MTN) cells and optimized their optical performance. Two-dimensional simulation reveals that the light leakage of the reverse tilt domain in MTN cells reduces the contrast and decreases the open ratio of the cell. We have proposed a novel method by applying a small bias voltage on the substrate, thus the light leakage can be suppressed and an open ratio of up to 89% can be achieved. As a result, properly designed MTN cells can achieve high resolution and high optical efficiency in reflective-type projection displays.

Acknowledgements

The authors wish to thank Dr. K. H. Yang, IBM T. J. Waston Research Center, Yorktown Heights, New York, U. S. A., for the suggestion of the topics. This work is supported by the National Science Council, Taiwan, Rep. of China, under contract number NSC85-2215-E-009-015.

References

[1] J. Glueck, H. U. Lauer, E. Lueder, T. Kallfass and D. Straub, SID'93 Digest, 299 (1993).
[2] J. De Baets, A. Van Calster, H. De Smet, J. Van Den Steen, G. Van Doorselaer, D. Wojciechowski, G. Schols and J. Witters, Asian Display'95, 477 (1995).
[3] S. T. Wu and C. S. Wu, to be published, SID'96 Proc.
[4] S. Dickmann, J. Eschler, O. Cossalter and D. A. Mlynski, SID'93 Digest, 638 (1993).
[5] K. W. Lin and H. P. D. Shieh, *Appl. Phys. Lett.*, **68**, 17 (1996).
[6] C. Gu and P. Yeh, *J. Opt. Soc. Am. A*, **10**, 966 (1993).
[7] H. L. Ong, *Appl. Phys. Lett.*, **51**, 18 (1987).